Calibration of the 3-PRS Parallel Manipulator Using a Motion Capture System

C. G. van Driel[1], J. A. Carretero[2]

[1] *University of New Brunswick, Dept of Mechanical Engineering, c.vandriel@unb.ca,*

[2] *University of New Brunswick, Dept. of Mechanical Engineering, Juan.Carretero@unb.ca*

In this paper, a kinematic calibration method for the 3-PRS parallel manipulator using a motion capture system is presented. Although parallel mechanisms present numerous advantages over their serial counterparts, an accurate kinematic model must be developed to facilitate their operation. Kinematic calibration is used to accurately determine the kinematic parameters of the kinematic model to improve the overall accuracy of the mechanism. The kinematic calibration of the 3-PRS parallel manipulator will be examined by identification of the manipulator's kinematic parameters, an introduction to the motion capture system used, and the presentation of the calibration method itself. For preliminary testing purposes, a virtual model of the manipulator has been generated in CAD. As the controller for the physical 3-PRS manipulator is under construction, the virtual model will be used to validate the method. The calibration method initially determines the joint locations and orientations, from which the remaining kinematic parameters can be resolved. Preliminary testing using the virtual model indicates the method is valid and can accurately determine the modeled parameters. Once the physical manipulator is operational, alterations the calibration method will be required to account for manufacturing and assembly tolerances/errors, joint offsets and noise during the static captures.

1 INTRODUCTION

For many applications of parallel mechanisms, the accuracy of the mechanism is of the utmost importance. As parallel manipulators are known for their high stiffness and payload capacity, low inertia effects (with actuators located at the base), and improved repeatability over serial manipulators [1], it is desired to have their accuracy approach their repeatability. In order to improve the accuracy of the mechanism, a kinematic calibration is used to determine its actual kinematic parameters. Utilizing the calculated parameters to modify the kinematic model, improvements in the mechanism's accuracy can be achieved.

The calibration of serial and parallel mechanisms is not a new concept. General overviews [2] and discussions [3] have been completed in the past to outline general advancements and techniques in the field. The kinematic parameters to be used are usually identified by intuition, while Besnard and Khalil [4] have developed a numerical method to assist in the identification of these parameters for parallel mechanisms.

Many approaches have been taken to refine the kinematic parameters, all of which have proven successful. Self-calibration is one technique that incorporates the use of redundant sensors on passive joints of the mechanism [5]. An alternative self-calibration was proposed in [6] by way of mechanical constraints imposed on the branches of the mechanism. Self-calibration techniques relieve the use of external sensors or cameras, but require the installation of sensors on passive joints during construction [5] or locking mechanisms on joints and the ability for actuated joints to be operated passively [6].

A common operation performed during calibration is the introduction of objective or error functions to account for the variance in joint parameters. Notash and Podhorodeski [7] make use of such operations in the kinematic calibration of three-branch parallel manipulators. Masory et al. [8] were responsible for a kinematic calibration on the six degree-of-freedom Stewart-Gough platform. More recently, Renaud et al. [9] introduced the use of vision-based kinematic calibration as a method of external sensing.

In this paper, a calibration method for the 3-$\underline{P}$RS manipulator using a motion capture system is introduced ($\underline{P}$ indicates the joint of actuation). The 3-$\underline{P}$RS was initially introduced by Carretero et al. [10] and has been examined by a variety of other researchers since [11-13]. The use of a motion capture system removes the need of an external fixture for calibration and does not require the installation of redundant sensors on passive joints. On the other hand, the system requires the attachment of a number of reflective markers, but their position and method of attachment is arbitrary. Each component of the manipulator can therefore be represented by these markers. The kinematic parameters can be determined from manipulation of the markers motion for a sequence of static captures.

This paper is organized into six sections. The first section introduces the 3-$\underline{P}$RS manipulator and its kinematic parameters. Section 2 includes an introduction to motion capture systems and a detailed examination of the system used for this calibration. The third section presents the calibration method, broken into three phases. The final three sections describe an experimental validation using a virtual model, a discussion on future work, and concluding remarks, respectively.

2 Manipulator Kinematics

The 3-$\underline{P}$RS manipulator is a three degree-of-freedom parallel manipulator whose kinematic architecture is presented in Figure 1. The 3-$\underline{P}$RS is characterized by a moving platform connected to a stationary base by three identical branches. Each branch contains an actuated prismatic joint at the base, a revolute joint, and a spherical joint attaching the fixed-length leg to the moving platform. The axis of the revolute joint is parallel to the base frame and perpendicular to the translational axis of the prismatic joint. This architecture permits orientation of the moving platform about two perpendicular axis, centered and parallel to the end effector frame, and elevation in the vertical axis of the base frame. It should be noted that there are extraneous translations in the horizontal plane that are pose dependant (described as 'parasitic motion' in Carretero et al. [14]).

As calibration seeks to refine the kinematic parameters of a manipulator, in order for a more accurate representation, it is imperative to identify all parameters that will require refinement. In an ideal case, depicted in Figure 1, the parameters that are of importance are: the individual joint locations and orientations, the leg length and the radius of the moving platform. The ideal case is absent of any manufacturing tolerances, assembly discrepancies, or joint offsets (including backlash). Representation of joint locations and orientations are

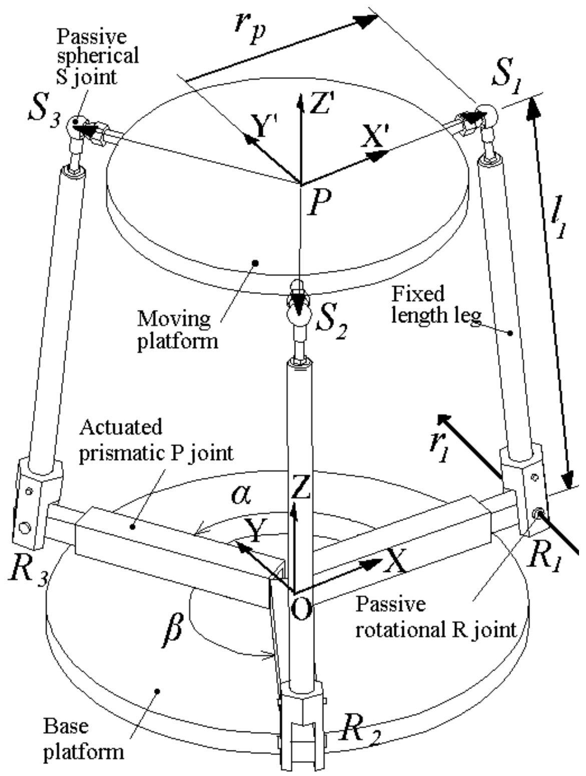

Figure 1: The 3-PRS parallel manipulator - Mechanism architecture and vector model from Carretero et al. [14]

dependant on the type of joint. Prismatic joints are represented by a unit vector parallel to the actuation direction, s_{p_i}. Revolute joints are represented by a unit vector in the direction of the axis of rotation s_{r_i} and a point on the axis, R_i. Spherical joints are represented by a single point corresponding to its centre, S_i. The angles between consecutive prismatic joints, α and β, can be determined by the prismatic joints' unit vectors. The radius of the end effector, r_p, is the distance from the end effector centre to the spherical joint centres. The leg length, l_i, is the distance between the spherical joint centre and the revolute joint axis.

Based on the architecture presented in Figure 1, a physical 3-PRS manipulator has been constructed. Figure 2 presents a CAD rendering of the constructed manipulator and indicates the location of the parameters detailed above. The physical manipulator has added parameters based on its fabrication and assembly, most notably joint offsets that will require determination. Since no joint can be constructed perfectly, each joint also has an associated error in its position and orientation. Similarly, if the joints are subjected to these errors, basing the calculation of other parameters on their position and orientation introduces cumulative errors. At present, the controller for the physical model is under development, that is, the manipulator can not be used for testing.

To overcome the added parameters associated with the physical manipulator and begin developing the calibration method, the CAD model presented in Figure 2 can be used. By using a virtual model, an ideal case is created where manufacturing and assembly issues,

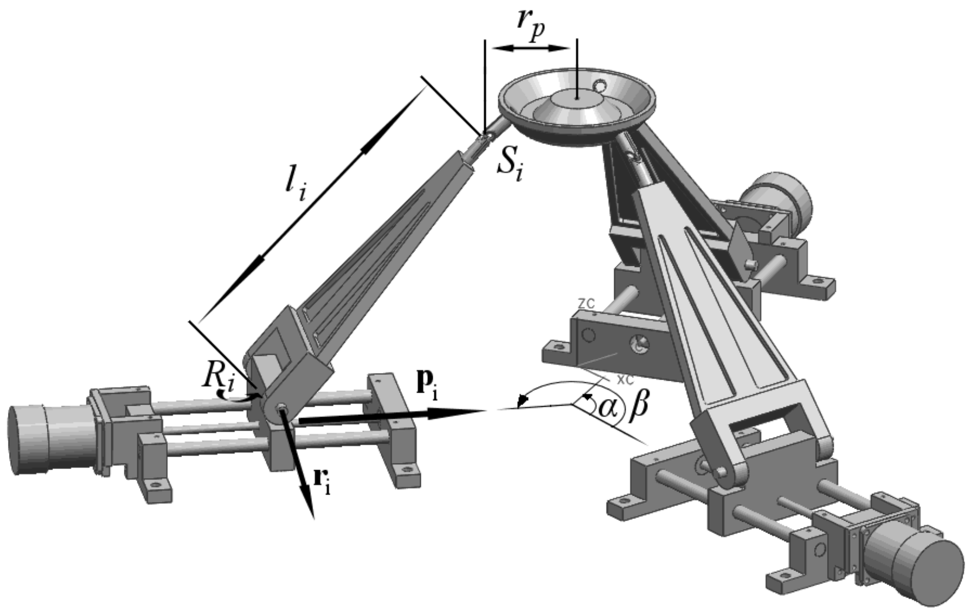

Figure 2: The 3-PRS parallel manipulator - CAD representation of physical construction.

as well as joint offsets/errors, can be eliminated. Using this model, preliminary testing can allow for verification of the calibration method in its simplest form. More advanced testing can also be completed by altering the model to include tolerance, assembly and joint issues on a gradual basis; in effect, growing the method by accounting for one parameter at a time. Once the physical model is operational, the CAD model can be used for comparison.

3 MOTION CAPTURE SYSTEMS

Motion capture systems are presently in widespread use in areas of computer and television animation, life sciences, and engineering. A number of manufacturers are available in today's market place to supply motion capture cameras and equipment. These include, but are not limited to: Vicon Motions Systems Ltd., Motion Analysis Corp., Peak Performance Technologies, Qualisys, and Visual 3D. Systems can vary in the marker identification methods (reflective or LED markers), precision of the camera's sensor and capture frame rate, to name a few.

For this calibration apparatus, eight Vicon VCam's are used for reflective marker capturing. Each VCam is equipped with a 659×493 pixel digital CMOS sensor, an infra-red strobe light and a frame rate of up to 200 frames per second.

Use of any motion capture system requires calibration in order to ensure overall precision based on camera locations. The Vicon cameras require a two step calibration process: one static and one dynamic capture. Use of this calibration method allows the Vicon system to obtain marker coordinates independent of camera locations through their proprietary algorithms. Static calibration is completed using an L-shaped calibration reference object. Based on the location of markers on the reference object, the software is able to establish a reference frame in the capture volume. Dynamic calibration is completed using a 'dynamic wand' which is waved throughout the capture volume. The wand contains two markers at a known distance, and is used to verify the precision of the camera setup. Vicon encourages each laboratory to perform their own measurements to the precision of the Vicon equipment; because it varies with ambient light levels, volume size, calibration, number of cameras, and reconstruction parameters imbedded in the software, the exact precision of any camera setup can not be stated.

With all manipulator calibration techniques, an avenue to extract data from the manipulator's pose is required. In the case of still images from an SLR or digital camera, image processing is required to determine the pose of the manipulator. Using the Vicon system, markers are attached to the rigid bodies comprising the manipulator. For each pose, the markers positions relative to the reference frame are determined, and can be extracted. As with most methods of image capturing, there is an associated noise with the data extraction. That is, with a high precision capture, no two captures/frames are the same. To account for this variation, static captures are used with a frame rate of 60 Hz for two seconds, or 120 frames per capture. Extracting a large number of frames for each static capture, permits an opportunity to limit the effect of noise in the capture. All data analysis is presently completed offline during post-processing.

Without an established precision for the system, a validation of the precision is required for any given setup. Using the Vicon system, a preliminary analysis was preformed to determine the range of precision that could be expected for a small volume capture. In this case, two setups for testing were used. The primary test was completed using eight cameras in a circular arrangement of varying heights around a marker setup. A secondary test was performed using only three cameras aligned with the axis of a Cartesian coordinate frame with the same marker setup. Initial results indicate that the variation on the markers position of at most $\pm$ 0.2 mm can be expected. Since this is an ideal case with all cameras having clear visibility of the markers, more tests are required when the manipulator's position and orientation with respect to the cameras is finalized.

4 CALIBRATION METHOD

The method of calibration used to determine the kinematic parameters of the 3-$\underline{P}$RS manipulator CAD model is outlined here. The first two phases (I & II) can be performed in any order, that is, one is independent of the other (thereby limiting any cumulative error). On the other hand, the last phase, Phase III, needs the results of the first two.

In Phase I, the axes of action of the revolute and prismatic joints are determined for each leg simultaneously. The second phase presents the method of determining the spherical joint centres. The final phase is completed using the parameters ascertained in phases one and two. Here the radius of the moving platform, leg lengths, and angles between the actuators are determined. In later versions of the method, any additional kinematic parameters will be solved for in this phase as well.

For calibration purposes, at least one marker must be located on each movable part of the manipulator. It should be noted that markers can be attached in any position or fashion, as long as it can be verified that the markers do not move, relative to their original point on the link, during the series of captures and are visible to at least two cameras. Although only one marker is required, increasing the number of markers used per moving part will improve the accuracy of the calculations. Figure 3 depicts an arbitrary location for the

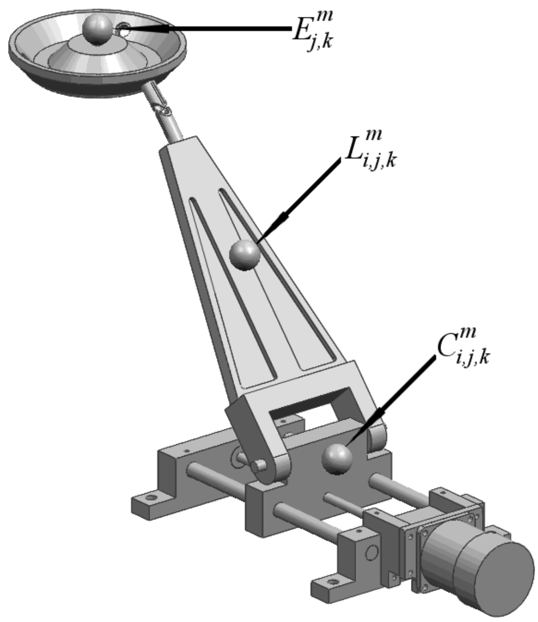

Figure 3: One leg of the 3-PRS manipulator - Arbitrary location of markers for calibration method.

markers on one of the legs. Markers are designated by either E, L, or C, for end effector, leg and carriage respectively. A superscript of m is to define the coordinates as those of a marker. Subscripts i, j, and k determine the leg number, marker index (if more than one mark is used per designation), and static capture number, respectively.

4.1 Phase I

This phase requires the prismatic joints to displace their entire travel. This is accomplished by raising the end effector from its minimum to its maximum elevation. In doing so, the legs attached to the prismatic joints will rotate from a position close to horizontal, to a position close to vertical (given the physical and singular limitations of the manipulator). This motion encompasses the largest work envelope for both the revolute and prismatic joints.

Presently, static captures are used to determine the marker locations for any given pose. That is, the motion required by each phase needs to be divided into multiple static captures, n. For calibration purposes, it can be shown that at least three static captures are required $n \geq 3$, preferably including both extremes of the work envelope. By increasing the number of static captures, the accuracy of the calculations can also be increased.

4.1.1 Prismatic joint axis

The marker located on the carriage of the prismatic joint $C^m_{i,j,k}$, for each capture k, traces a path in the axis of each prismatic joint $\mathbf{p}_{i,k}$. Using at least three data captures, the unit vectors, $\mathbf{s}_{p_i}$, in the direction of the three prismatic joints can be determined (for $i = 1, 2, 3$).

$$\mathbf{p}_{i,k} = C^m_{i,j,k+1} - C^m_{i,j,k} \tag{1}$$

$$\mathbf{s}_{p_i} = \frac{1}{n-1}\sum_{k=1}^{n-1}\frac{\mathbf{p}_{i,k}}{|\mathbf{p}_{i,k}|} \tag{2}$$

where i is the number of the leg ($i = 1, 2, 3$), j is the marker index, k is the number of the capture, n is the total number of captures, $\mathbf{p}_{i,k}$ is a vector coincident to the axis of the prismatic joint and $\mathbf{s}_{p_i}$ is the average unit vector calculated using the $n-1$ vectors $\mathbf{p}_i$.

4.1.2 Revolute joint axis and point

Using the marker located on the carriage of the prismatic joint as a reference, $C^m_{i,j,k}$, the marker data from each capture can be transformed to one of the known reference locations. That is, all markers on the leg, $L^m_{i,j,k}$, are transformed according to the displacement of the carriage. This allows the leg marker set to provide data for a pure rotation about the revolute joint axis. By creating vectors $\mathbf{v}_{i,j,k}$ between consecutive marker captures, the vector cross product can be used to determine the instantaneous axis of rotation of the leg with respect to the carriage. This axis is equivalent to the unit vector for the axis of rotation denoted by $\mathbf{s}_{r_i}$.

$$\mathbf{v}_{i,j,k} = L^m_{i,j,k} - (C^m_{i,j,k} - C^m_{i,j,k+2}) - L^m_{i,j,k+1}(C^m_{i,j,k+1} - C^m_{i,j,k+2}) \tag{3}$$

$$\mathbf{s}_{r_i} = \frac{1}{n-1}\sum_{k=1}^{n-1}\frac{\mathbf{v}_{i,j,k}\times\mathbf{v}_{i,j,k+1}}{|\mathbf{v}_{i,j,k}\times\mathbf{v}_{i,j,k+1}|} \tag{4}$$

Determining the middle point between two consecutive marker captures, $P^{\mathbf{v}}_{i,j,k}$ and using the vector $\mathbf{v}_{i,j,k}$ as a normal vector, $n-1$ planes can be formed, $\Lambda_{i,j,k}$.

$$P^{\mathbf{v}}_{i,j,k} = \frac{L^m_{i,j,k} + L^m_{i,j,k+1}}{2} \tag{5}$$

$$\Lambda_{i,j,k} : \mathbf{v}^T_{i,j,k}A_i = \mathbf{v}^T_{i,j,k}P^{\mathbf{v}}_{i,j,k} \tag{6}$$

All $\Lambda_{i,j,k}$ planes will generate a line of intersection coincident with the axis of revolution. Using the vector equation definition of a plane, an arbitrary point, A_i, in the xz-plane of the base frame, Λ_{XZ}, can be determined by solving for the intersection of the planes $\Lambda_{i,j,k}$, and the xz-plane Λ_{XZ}.

$$A_i = \begin{bmatrix} \mathbf{v}^T_{i,j,k} \\ \mathbf{v}^T_{i,j,k+1} \\ 0\ 1\ 0 \end{bmatrix}^{-1} \begin{bmatrix} P^{\mathbf{v}}_{i,j,k}\mathbf{v}_{i,j,k} \\ P^{\mathbf{v}}_{i,j,k+1}\mathbf{v}_{i,j,k+1} \\ 0 \end{bmatrix} \tag{7}$$

Applying $\mathbf{s}_{r_i}$ to A_i, the axis of rotation, $\mathbf{r}_i$ can be resolved.

$$\mathbf{r}_i = A_i + k\mathbf{s}_{r_i} \tag{8}$$

4.2 Phase II

This phase requires only one prismatic joint to displace its maximum travel (limited by singular configurations) while the other prismatic joints are held in place. The two stationary prismatic joints are to be held in the approximate centre of their possible travel. The free prismatic joint will travel to its maximum and minimum allowable positions. This process is repeated for each leg in three separate sessions, $l = 1, 2, 3$. As in the previous phase, it can be shown that at least three static captures are required per session $n \geq 3$, preferably including both extremes of the end effector work envelope.

4.2.1 Spherical joint center

For each leg session, Phase I equations (3) to (8) can be repeated to determine the axis of rotation for the end effector. With two legs stationary, the line $\mathbf{r}_l$ determined is a line coincident to the vector between the two stationary spherical joint centres.

$$\begin{aligned} \mathbf{r}_l &= A_l + k_l \mathbf{s}_{r_l} \\ \mathbf{r}_{l+1} &= A_{l+1} + k_{l+1} \mathbf{s}_{r_{l+1}} \end{aligned} \tag{9}$$

Using the line from the three sessions, a triangle of lines can be generated whose vertices represent the spherical joint centres S_i.

$$A_l + k_l \mathbf{s}_{r_l} = A_{l+1} + k_{l+1} \mathbf{s}_{r_{l+1}} \tag{10}$$

$$k_l = \frac{\left|(A_{l+1} - A_l) \times \mathbf{s}_{r_{l+1}}\right|}{\left|\mathbf{s}_{r_l} \times \mathbf{s}_{r_{l+1}}\right|} \tag{11}$$

$$S_i = A_l + k_l \mathbf{s}_{r_l} \tag{12}$$

4.3 Phase III

This phase is completed using the parameters determined in Phases I & II. With the joint positions and orientation known, the remaining kinematic parameters can be solved for.

4.3.1 Platform radius

The spherical joint centres can be used to determine the end effector centre, P and platform radius, r_p. The radius is the magnitude of the vector between the centre, P and one of the spherical joint centers, S_i.

$$P = \frac{1}{3}\sum_{i=1}^{3} S_i \tag{13}$$

$$r_p = P - S_i \tag{14}$$

4.3.2 Leg length

Leg length, l_i can be determined from the shortest distance between any leg's spherical joint centre, S_i and its revolute joints axis of rotation, $\mathbf{r}_i$. Using the arbitrary point on the revolute axis, A_i, and S_i, a projection can be made onto the revolute axis to determine the leg length.

$$\mathbf{a}_i = S_i - A_i \tag{15}$$

$$l_i = |\mathbf{a}_i \times \mathbf{s}_{r_i}| \tag{16}$$

where $\mathbf{a}_i$ is the vector between the arbitrary point A_i and spherical joint centre S_i.

4.3.3 Prismatic joint orientation

The angles α and β between the three prismatic joints can be determined by the dot product of their axis unit vectors determined in equation (2).

$$\alpha = \arccos\left(\mathbf{s}_{p3} \cdot \mathbf{s}_{p1}\right) \tag{17}$$

$$\beta = \arccos\left(\mathbf{s}_{p2} \cdot \mathbf{s}_{p1}\right) \tag{18}$$

Completing all phases of the calibration fully defines all kinematic parameters for the virtual 3-PRS manipulator.

5 EXPERIMENTAL VALIDATION

As mentioned in the manipulator kinematics section, an ideal 3-PRS manipulator has been modeled in CAD. The model is an ideal form of the physical manipulator, and does not represent the manufacturing, assembly or joint tolerances/errors. Using this model, it is possible to verify the calibration method in its preliminary form. Through the CAD model it is possible to obtain any feasible manipulator pose based on physical mating conditions of the manipulator's components. By attaching virtual spherical markers resembling those of the Vicon system, the exact marker centre locations can be extracted using the software. Figure 4 indicates the marker locations used on the virtual manipulator. Presently three markers are used on the end effector and three more on each leg, $j = 3$. Two markers are attached to the carriage of each of the prismatic joints, $j = 2$, and two more markers are used as stationary references on the base of each prismatic joint (not required in present calibration). When testing begins on the physical 3-PRS, more markers may be used to improve the accuracy of the parameter calculation.
Applying the calibration method outlined in the previous section, five captures were used in both phases of data acquisition, that is, $k = 5$. The architectural parameters used for the virtual 3-PRS are listed in Table 1 along with the parameters determined by the calibration. An exact match was predicted, and proves that in the ideal situation, the method is appropriate and accurate.

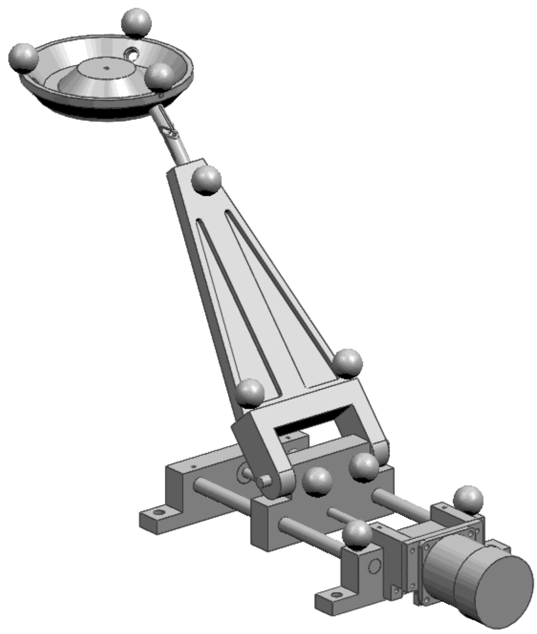

Figure 4: One leg of the 3-PRS manipulator - Location of virtual markers for preliminary testing.

Parameter	CAD Model	Calibration results
$\mathbf{s}_{p_1}$	$\begin{bmatrix} -1 & 0 & 0 \end{bmatrix}^T$	$\begin{bmatrix} -1 & 0 & 0 \end{bmatrix}^T$
$\mathbf{s}_{p_2}$	$\begin{bmatrix} 0.5 & 0.8660 & 0 \end{bmatrix}^T$	$\begin{bmatrix} 0.5 & 0.8660 & 0 \end{bmatrix}^T$
$\mathbf{s}_{p_3}$	$\begin{bmatrix} 0.5 & -0.8660 & 0 \end{bmatrix}^T$	$\begin{bmatrix} 0.5 & -0.8660 & 0 \end{bmatrix}^T$
$\mathbf{s}_{r_1}$	$\begin{bmatrix} 0 & 1 & 0 \end{bmatrix}^T$	$\begin{bmatrix} 0 & 1 & 0 \end{bmatrix}^T$
$\mathbf{s}_{r_2}$	$\begin{bmatrix} -0.8660 & 0.5 & 0 \end{bmatrix}^T$	$\begin{bmatrix} -0.8660 & 0.5 & 0 \end{bmatrix}^T$
$\mathbf{s}_{r_3}$	$\begin{bmatrix} 0.8660 & 0.5 & 0 \end{bmatrix}^T$	$\begin{bmatrix} 0.8660 & 0.5 & 0 \end{bmatrix}^T$
A_1	$\begin{bmatrix} 344.545 & 0 & 0 \end{bmatrix}^T$	$\begin{bmatrix} 344.545 & 0 & 0 \end{bmatrix}^T$
A_2	$\begin{bmatrix} -689.09 & 0 & 0 \end{bmatrix}^T$	$\begin{bmatrix} -689.09 & 0 & 0 \end{bmatrix}^T$
A_3	$\begin{bmatrix} -689.09 & 0 & 0 \end{bmatrix}^T$	$\begin{bmatrix} -689.09 & 0 & 0 \end{bmatrix}^T$
S_1	$\begin{bmatrix} 82.8996 & 0 & 230.9006 \end{bmatrix}^T$	$\begin{bmatrix} 82.8996 & 0 & 230.9006 \end{bmatrix}^T$
S_2	$\begin{bmatrix} -41.4498 & -71.7953 & 230.9006 \end{bmatrix}^T$	$\begin{bmatrix} -41.4498 & -71.7953 & 230.9006 \end{bmatrix}^T$
S_3	$\begin{bmatrix} -41.4498 & 71.7953 & 230.9006 \end{bmatrix}^T$	$\begin{bmatrix} -41.4498 & 71.7953 & 230.9006 \end{bmatrix}^T$
l_1	306.555	306.555
l_2	306.555	306.555
l_3	306.555	306.555
r_p	82.8996	82.8996
α	120.0000	120.0000
β	240.0000	240.0000

Table 1: Calibration results compared to the model for all kinematic parameters.

6 Future Work

Virtual calibration was the first step in the calibration method's creation. Once the physical 3-PRS is operational, alterations to the calibration method may be required due to an increase in kinematic parameters. The required number of kinematic parameters will increase to accommodate the additional complexity of fabrication, assembly and joint tolerances/errors. Due to the increase in kinematic parameters additional poses and/or captures may be required to determine a solution. Noise in the capture data will also lead to variation in the calculations that will not produce perfect results (e.g. in the case of intersecting lines and planes). All required alterations will be processed on an individual basis to provide an appropriate solution for the method.

7 Conclusions

A proposed calibration method for the 3-PRS parallel manipulator using a motion capture system was presented in this paper. The kinematic architecture of the manipulator was discussed along with an introduction to the fabricated manipulator. As the manipulator is not operational, a virtual model was generated in CAD to its likeness. The proposed method is a preliminary calibration strategy for use with the virtual model. The calibration method is able to determine the manipulators joint locations and orientations based on marker locations captured from a motion capture system (emulated using CAD software). Using the joint parameters, the remaining kinematic parameters can be geometrically determined. Although limited by software precision, applying the method to the virtual model yielded results equivalent to the true kinematic parameters of the model. Using the preliminary results as a foundation, alterations will be made to the calibration method to reflect the complex nature of the fabricated manipulator.

Bibliography

[1] Tsai, L.W., Robot Analysis - The mechanics of serial and parallel manipulators, New York, NY: John Wiley & Sons, 1999.

[2] Roth, Z. S., Mooring, B. W., and Ravani, B., An Overview of Robot Calibration, IEEE Journal of Robotics and Automation, **3**(5):377-385, 1987.

[3] Zou, H., and Notash, L., Discussions on the Camera-Aided Calibration of Parallel Manipulators, Procedings of 2001 CCToMM Symposium on Mechanisms, Machines, and Mechatronics, June 1, 2001, Saint-Hubert (Montréal), Québec.

[4] Besnard, S., and Khalil, W., Identitfiable Parameters for Parallel Robots Kinematic Calibration, Proceedings of 2001 IEEE: International Conference on Robotics and Automation, May 21-26, 2001, Seoul, Korea.

[5] Zhuang, H., and Lui, L., Self-Calibration of a Class of Parallel Manipulaotrs, Proceedings of 1996 IEEE: International Conference on Robotics and Automation, April 22-28, 1996, Minneapolis, Minnesota.

[6] Khalil, W., and Besnard, S., Self-Calibration of Stwart-Gough Parallel Robots Without Extra Sensors, IEEE Transactions on Robotics and Automation, **15**(6):1116-1121, 1999.

[7] Notash, L., and Podhorodeski, R., Kinematic Calibration of Parallel Manipulators, Proceedings of 1995 IEEE: International Conference on Systems, Man and Cybernetics, Oct 22-25, 1995, Vancouver, British Columbia.

[8] Masory, O., Wang, J., and Zhuang, H., On the Accuracy of the Stewart Platform - Part II Kinematic Calibration and Compensation, Proceedings of 1993 IEEE: International Conference on Robotics and Automation, May 2-6, 1993, Atlanta, Georgia.

[9] Renaud, P., Andreff, N., Marquet F., and Martinet, P., Vison-based Kinematic Calibration of a H4 Parallel Mechanism, Proceedings of 2003 IEEE: International Conference on Robotics and Automation, September 14-19, 2003, Taipei, Taiwan.

[10] Carretero, J., Podorodeski, R., Nahon, M., and Gossein, C., Kinematic Analysis and Optimization of a new three degree-of-freedom spatial parallel manipulator, Journal of Mechanical Design, **122**(1):17-24, 2000.

[11] Pond, G., and Carretero, J., Kinematic Analysis and Workspace Determination of the Inclined $\underline{\text{P}}$RS Parallel Manipulator, Proceedings of RoManSy 2004: 15th CISM-IFToMM Symposium on Robot Design, Dynamics and Control, June 14-18, 2004, Montreal, Canada.

[12] Yangmin, L., and Qingsong, X., Kinematic and Stiffness Analysis for a General 3-$\underline{\text{P}}$RS Spatial Pallel Manipulator, Proceedings of RoManSy 2004: 15th CISM-IFToMM Symposium on Robot Design, Dynamics and Control, June 14-18, 2004, Montreal, Canada.

[13] Tsai, M., Shiau, T., Tsai, Y., and Chang, T., Direct Kinematic Analysis of a 3-PRS Parallel Mechanism, Mechanism and Machine Theory, **39**(1):71-83, 2003.

[14] Carretero, J., Nahon, M., and Podorodeski, R., Workspace Analysis and Optimization of a Novel 3-DOF Parallel Manipulator, International Journal of Robotics and Automation, **15**(4):178-188, 2000.